Influence of Li-ion Battery Models in the Sizing of Hybrid Storage Systems with Supercapacitors

Pinto, Claudio; Barreras, Jorge Varela; de Castro, Ricardo; Schaltz, Erik; Andreasen, Søren Juhl; Araujo, Rui Esteves

Published in:
Proceedings of the 2014 IEEE Vehicle Power and Propulsion Conference (VPPC)

DOI (link to publication from Publisher):
10.1109/VPPC.2014.7007090

Publication date:
2014

Document Version
Early version, also known as pre-print

Influence of Li-ion Battery Models in the Sizing of Hybrid Storage Systems with Supercapacitors

Cláudio Pinto*, Jorge V. Barreras‡, Ricardo de Castro†, Erik Schaltz‡, Søren J. Andreasen‡, Rui Esteves Araújo*
*INESC TEC (formerly INESC Porto) and Faculty of Engineering, University of Porto, Porto, 4200-465, Portugal
†Institute of System Dynamics and Control, Robotics and Mechatronics Center
German Aerospace Center (DLR), Wessling, D-82234, Germany
‡Department of Energy Technology, Aalborg University, Aalborg, 9220, Denmark
Email: dee12015@fe.up.pt, jvb@et.aau.dk, Ricardo.DeCastro@dlr.de, esc@et.aau.dk, sja@et.aau.dk, raraujo@fe.up.pt

***Abstract*—This paper presents a comparative study of the influence of different aggregated electrical circuit battery models in the sizing process of a hybrid energy storage system (ESS), composed by Li-ion batteries and supercapacitors (SCs). The aim is to find the number of cells required to propel a certain vehicle over a predefined driving cycle. During this process, three battery models will be considered. The first consists in a linear static zeroeth order battery model over a restricted operating window. The second is a non-linear static model, while the third takes into account first-order dynamics of the battery. Simulation results demonstrate that the adoption of a more accurate battery model in the sizing of hybrid ESSs prevents over-sizing, leading to a reduction in the number of cells of up to 29%, and a cost decrease of up to 10%.**

I. Introduction

Due to well-known limitations of ESS's for electric vehicles (EVs) - such as high cost, modest power and energy densities-, in recent years, there has been an increased interest in developing storage systems with multiple storage technologies (batteries, fuel cells and SCs) [1]–[3]. From the several possible combinations, our interest will lie on the hybridization of batteries and SCs. Previous research on this topic concluded that, by a careful selection of batteries and SCs, such hybrid ESS can provide, not only lower installation costs when compared to the use of a single-source ESS, but also lower energy consumption and stress reduction in the main source [3].

In the literature we can easily find sizing or energy management strategies based on simple heuristics [8] or machine learning [5] techniques, while others use optimal control methods [6], [9]. This latter approach considers problems that can provide the global optimal solution. However, frequently, simplifications are required and certain characteristics assumed, such as linear voltage dependency or constant inner resistance, which leads to models that may not describe very accurately the ESS. These simplifications are generally justified at early stages of the system design process or whenever low computational complexity or low configuration effort is required [6], [9]. Nonetheless, it is important to have in mind that these simplifications carry with them approximation errors. One of the main goals of this work is to investigate the effect of such approximations is the sizing of hybrid ESS, which, to the best of our knowledge, was not investigated in previous research.

Nowadays an abstract approach is commonly used in literature for sizing problem of hybrid e-mobility applications: aggregated battery pack Equivalent Circuit Models (ECMs) are proposed, based on a linear static zeroeth order single cell ECM, over a restricted operating window (e.g. 5-95% SoC), without taking into account statistical data on cell-to-cell variation [1], [2], [7].

In this paper, the obtained results using the aforementioned modelling approach are compared with two other battery models, non-linear static zeroeth order model and non-linear dynamic first order model, in order to evaluate from a qualitative point of view the influence of the battery model complexity into the sizing problem. Additionally, we also propose an algorithm that relies on low/high pass filters for the power allocation and consequently the sizing problem of the ESS, which represents a realistic allocation strategy [2], [4], [7]. The main advantage of this strategy is the ability to handle the different ESS models, without requiring significant model simplifications.

II. ESS Model

A. Mathematical Model

The models of the ESS's cells considered in this work are represented through Equivalent Circuit Models (ECMs) [3], [10]–[12], see Fig. 1. These ECMs are mathematically characterized as:

$$v_j(t) = OCV_j(q_j(t)) - \Delta v_j(t), \quad j \in \mathcal{M} \tag{1a}$$

$$q_j(t) = \frac{1}{\overline{Q}_j}\int_0^t i_j(\delta)d\delta + q_j(0) \tag{1b}$$

where v_j is the output voltage of the cell, OCV_j the cell's open-circuit voltage, and Δv_j the voltage drop in the cell's internal impedance. The state of charge (SoC) is given by q_j, the maximum charge of the cell by $\overline{Q}_j$, and the cell's current by $i_j(\in \mathbb{R})$. Normally, the current, the SoC and the terminal voltage of the cell are constrained by physical limits:

$$i_j^{min} \leq i_j(t) \leq i_j^{max} \tag{2a}$$

$$q_j^{min} \leq q_j(t) \leq q_j^{max} \tag{2b}$$

$$v_j^{min} \leq v_j(t) \leq v_j^{max} \tag{2c}$$

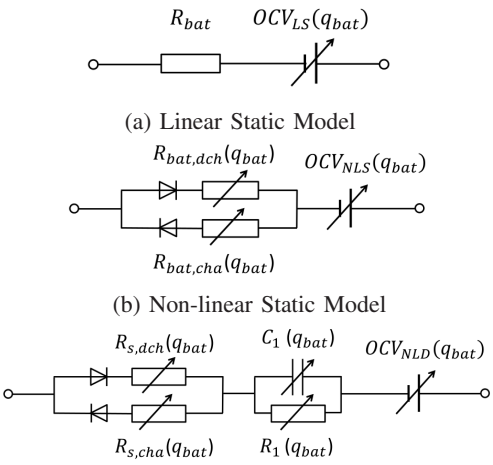

(a) Linear Static Model

(b) Non-linear Static Model

(c) Non-linear Dynamic Model

Fig. 1: ESS's Equivalent Circuit Models

which are presented in Table I and Table II for both sources. In the sequel, four sets of cell's models $\mathcal{M} = \mathcal{B} \cup \{SC\} = \{LS, NLS, NLD, SC\}$ will be considered. The first three are battery models, while the last one is related with SCs.

Linear Static Model ($j = LS$) The first battery model assumes linear OCV and a constant internal resistance of the cell. It is defined as:

$$OCV(t) = a + b.q(t) \tag{3}$$
$$\Delta v(t) = R_{bat} i(t) \tag{4}$$

where (a, b, R_{bat}) are parameters of the LS model. Notice that, in order to simplify the notation, the sub-indexes of the variables $(OCV, q, \Delta v, i)$ were omitted.

Non-Linear Static Model ($j = NLS$) The second model takes into account SoC-related nonlinearities in the OCV and in the internal resistance. These nonlinearities are approximated using piecewise linear (PWL) functions. In order to formulate the PWL approximation, let us divide the q range in N_p sub-intervals, $[\underline{q}_k, \overline{q}_k]$, $k \in [1, N_p]$ where $\underline{q}_k$ and $\overline{q}_k$ are the interval limits. Then,

$$OCV(t) = \sum_{k=1}^{N_p} (u_{0k} + u_{1k} q(t)) B(k, q(t)) \tag{5}$$
$$\Delta v(t) = R_{bat}(q(t)) i(t) \tag{6}$$
$$R_{bat}(q(t)) = \begin{cases} \sum_{k=1}^{N_p} (d_{0k} + d_{1k} q(t)) B(.) & \text{if } i(t) \geq 0 \\ \sum_{k=1}^{N_p} (c_{0k} + c_{1k} q(t)) B(.) & \text{if } i(t) < 0 \end{cases} \tag{7}$$

where u_{0k}, u_{1k}, d_{0k}, d_{1k}, c_{0k} and c_{1k} are parameters and $B(k, q)$ is an indicator function that returns 1 if $q \in [\underline{q}_k, \overline{q}_k]$ and 0 otherwise.

Non-linear Dynamic Model ($j = NLD$) The third model, besides SoC-related nonlinearities, also takes into account

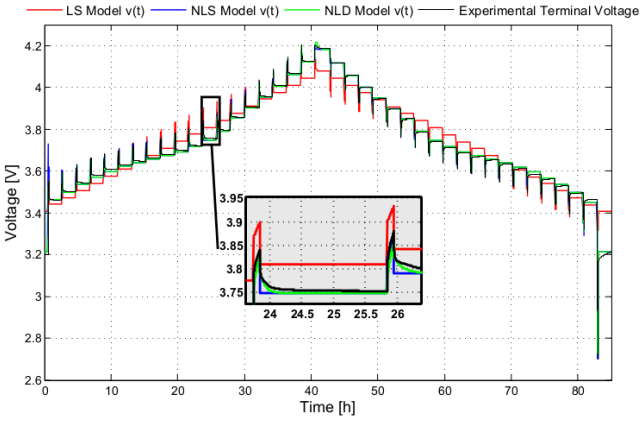

Fig. 2: Charging and discharging cycles for a single battery cell.

first-order dynamics in the ESS's cells

$$OCV(t) = \sum_{k=1}^{N_p} (u_{0k} + u_{1k} q(t)) B(k, q(t)) \tag{8}$$
$$\Delta v(t) = R_s(q(t)) i(t) + \Delta v_c(t) \tag{9}$$
$$\frac{d\Delta v_c(t)}{dt} = \frac{1}{C_1(q(t))} \left(i(t) - \frac{\Delta v_c(t)}{R_1(q(t))} \right) \tag{10}$$

In the above representation, the variables $R_s(q(t))$, $C_1(q(t))$, $R_1(q(t))$ are approximated by PWL function similar to (7). Yet, C_1 and R_1 will assume discharging values when $\Delta v_c(t) > 0$ and charging values otherwise.

Supercapacitors ($j = SC$) The supercapacitors are modelled using a similar structure to the LS representation of the battery:

$$OCV(t) = \frac{\overline{Q}_{SC}}{C} q(t) \tag{11}$$
$$\Delta v(t) = R_{SC} i(t) \tag{12}$$

where $\overline{Q}_{SC}$ represents the nominal charge of the SC, C the capacitance of the SC, and R_{SC} the internal resistance.

B. Parametric Identification

The parameterization of the Li-ion battery ECMs was based on capacity check and step response tests conducted on an unused and relatively new Kokam SPLB 120216216 Li-ion pouch cell. All tests were conducted at 0.5C (26.5A) and 25°C. First of all a full charge and discharge cycle was conducted in order to estimate charging and discharging capacity. Using this information, the battery tester was programmed to fully charge and discharge the cell in consecutive steps of 5% SoC, considering a 2h relaxation period between pulses. Thus the OCV vs SoC charging and discharging characteristics are obtained. Since an insignificant hysteresis effect is observed (Fig. 2), the average OCV vs SoC characteristic is considered for linear and non-linear fitting. Then, using the same experimental data, the charging and discharging resistances are calculated for every 5% SoC step depending on the ECM. Either an average value

TABLE I: BATTERY PARAMETERS [per cell]

Kokam SLPB 120216216			
Variable	Symbol	Value	Unit
Pouch Cell Mass	$m_{PC,bat}$	1.2	kg
Total Cell Mass	m_{bat}	1.83	kg
Nominal voltage	v_{bat}	3.7	V
Nominal capacity	$\overline{Q}_{bat}$	53	A.h
Initial capacity	$q_{bat}(0)$	0.95	-
SoC limits	$[q_{bat}^{min}, q_{bat}^{max}]$	[0.05,0.95]	-
Current limits	$[i_{bat}^{min}, i_{bat}^{max}]$	[-106,265]	A
Voltage limits	$[v_{bat}^{min}, v_{bat}^{max}]$	[2.7,4.2]	V
Cell Cost	c_{bat}	136	$
Search step	-	3	-

TABLE II: SUPERCAPACITOR PARAMETERS [per cell]

Maxwell BCAP0310 P270 T10			
Variable	Symbol	Value	Unit
Mass	m_{sc}	0.06	kg
Nominal voltage	v_{sc}	2.7	V
Capacitance	C_{sc}	310	F
Nominal capacity	$\overline{Q}_{SC}$	0.2325	A.h
Initial capacity	$q_{sc}(0)$	1	-
SoC limits	$[q_{SC}^{min}, q_{SC}^{max}]$	[0.5,1]	-
Current limits	$[i_{SC}^{min}, i_{SC}^{max}]$	[-250,250]	A
Internal resistance	R_{sc}	0.0022	$m\Omega$
Cell Cost	c_{SC}	8.3	$
Search step	-	5	-

is calculated (LS) according to Ohm's law or a non-linear fitting is conducted (NLS and NLD) [10]–[12].

From Fig. 2 it is evident that with higher model complexity, more accurate results are obtained. LS model not only presents a higher overall error, but also presents significant differences for certain SoC values, e.g. terminal voltages $v(t)$ in the charging process between 55% and 65% of SoC. The NLS and NLD models present more similar results, but the battery presents a dynamic effect not captured by the NLS model. In that sense, for the same required power different currents will be required leading to a performance of the system different from the real dynamic.

III. Sizing of the Hybrid ESS

The hybrid ESS, under consideration here, is composed by a battery pack and a SC pack. These packs are made up of a series of n_{SC} and n_{bat} cells (each cell weights m_j and costs c_j); it is also assumed that the two packs are connected to the DC-bus through two DC/DC converters, operating in parallel. The mass of the battery considers not only the mass of the pouch cell $m_{PC,bat}$, but also other elements such as cables, switch box, cooling system, etc. Due the simplicity and low weight of a singular SC cell that extra mass was neglected. The main goal of the hybrid ESS's sizing task consists in finding the number of cells of the two packs, n_j, that minimize a given cost function (to be introduced shortly), while fulfilling a set of technical constraints and requirements.

A. Output Power and Losses

With respect to the sizing requirements, we will consider that the hybrid ESS should be designed having in mind a pre-defined, deterministic, driving cycle, characterized by a speed profile $V(t), t \in [0, T_{DC}]$ and duration T_{DC}. Based on this information, together with the Newton's law, we can determine the vehicle's output power throughout the driving cycle:

$$P_{veh}(t) = \left(\frac{1}{2}\rho_a C_d A_f V(t)^2 + M\left(g f_r + \frac{dV(t)}{dt}\right)\right) V(t) \quad (13)$$

where g is the gravity acceleration constant, A_f is the vehicle frontal area, ρ_a is the air density, C_d is the aerodynamic drag coefficient and f_r is the rolling resistor coefficient. The first term is the power caused by the aerodynamic drag, and the second one depends on the rolling and inertial (respectively) resistance forces.

The vehicle mass M can be decomposed in two parcels:

$$M = m_0 + \sum_{j \in \mathcal{J}} m_j n_j \quad (14)$$

the first is associated with the vehicle mass without storage unit (m_0), while the second represents the contribution of the hybrid ESS (notice that $\mathcal{J}$ represents the storage units' sub-indexes employed in the hybrid ESS).

On top of the vehicle's output power P_{veh}, the sizing task should also take into account the losses in the vehicle's powertrain. In this work, it is assumed that the powertrain is composed by the following components: a mechanical transmission, an electric motor, two DC/DC converters and two ESS packs. To model the losses in these components, we adopted a similar approach to the one described in [3], which relies on the following considerations:

- The efficiency of the mechanical transmission is approximately constant.
- The electric motor losses can be approximated by polynomials dependent on the vehicle speed $V(t)$ and output torque;
- The DC/DC converter losses can be approximated by a quadratic polynomial dependent on the converter's current i_j.
- ESS's losses are dominated by the Ohmic losses in the ECMs.

These powertrain's losses can be compactly described by the non-linear function

$$P_l(t) = g_l(P_{veh}(t), V(t), i_j(t), n_j) \quad (15)$$

For the sake of brevity, the exact characterization of this function are omitted here (the interested reader is referred to [3] for additional details). For very high braking peak powers, mechanical brakes will dissipate the excess power $P_{brk}(t)$ that can not be absorbed by the ESS. The braking power is given by

$$P_{brk}(t) = \begin{cases} 0 & \text{if } P_{veh} \geq P_{reg}^{max} \\ P_{veh} - P_{reg}^{max} & \text{otherwise} \end{cases} \quad (16)$$

where P_{reg}^{max} is the maximum regenerative power of the ESS which depends on the ESS's state and size. Furthermore, the power losses caused by the radio, lights, HVAC and other loads, were considered constant during the driving cycle, such

that $P_a = 1$kW. Finally, the power provided by the hybrid ESS must be able to provide all the power needs of the vehicle:

$$P_{out}(t) = P_{veh}(t) + P_l(t) + P_a(t) - P_{brk}(t) = \sum_{j\in\mathcal{J}} n_j OCV_j(q_j(t))i_j(t) = \sum_{j\in\mathcal{J}} P_j(t) \quad (17)$$

B. Cost Functions

Two type of costs will be considered in the sizing process. The first is the installation cost of the cells:

$$J_{ins} = \sum_{j\in\mathcal{J}} c_j n_j \quad (18)$$

The second cost is related with charging costs of the ESS:

$$J_{run} = \gamma \int_0^{T_{dc}} P_{out}(t)dt \quad (19)$$

with $\gamma = N_{cycles} * C_e$, where N_{cycles} is the number of cycles expected that the battery accomplish and C_e is the energy cost [\$/Ws].

C. Problem Formulation

By combining the costs and the technical constrains presented above, we are now in conditions to pose the sizing problem:

$$\min_{i_j,n_j} J_{ins} + J_{run}$$
$$(1), (2), (13), (14), (15), (17) \quad (20a)$$
$$j \in \mathcal{J} \subset \mathcal{M} \quad (20b)$$

In the above representation, there are two important points that are worth discussing.

The first point is related with the fact that, besides sizing, the above problem also addresses the energy management of the hybrid ESS. In other words, we will need to find the optimal set of n_j (i.e., the sizing problem) and the current i_j of the two sources (i.e., the energy management problem).

The second noteworthy fact is the subset $\mathcal{J}$. As already mentioned, our interest here is related with the study of different battery models. Consequently, in the next section, three different $\mathcal{J}$ will be investigated: $\mathcal{J}_1 = \{LS, SC\}$, $\mathcal{J}_2 = \{NLS, SC\}$ and $\mathcal{J}_3 = \{NLD, SC\}$.

D. Pragmatic Solution

The main challenge in solving (20) lies in non-linearities present in the problem's constraints. In this article, we will follow a pragmatic approach to handle this problem. Our approach relies on two main steps. The first step is the discretization of the number of cells: $n_j \in \{n_j^0, n_j^1, \ldots, n_j^N\} = \mathcal{N}_j$. The second step consists in the adoption of a realistic, although non-optimal, energy-management strategy for the power split between batteries and supercapacitors. The idea is to employ a filter-based allocation policy. The motivation for this allocation policy is related to the complementary capabilities of the ESS's under consideration here. On one hand, the high peak power capability of the SCs makes this source ideal to handle the fast power transients. On the other hand, the batteries, with much higher energy density than SCs, are more suitable to provide the slower power variations, associated with the average energy needs for the vehicle motion. It is based on this line of reasoning that the frequency-based power allocation emerged in recent years as one of the simplest and most appealing strategies for the real-time managing of a hybrid ESS [2], [4], [7]. The implementation of this allocation policy is normally carried out with low/high pass filters, and uses the filter's time-constant τ as the main tuning parameter:

$$\tau \frac{d(P_{bat} - P_l^{bat})}{dt} + P_{bat} - P_l^{bat} = P_{out} - P_l^{SC} \quad (21)$$

where P_l^j represent the losses in the ESS pack and in its power converter. Given that the ideal value for the filter's time constant is unknown, we will treat τ as an additional decision variable in our combined sizing+energy management problem. This time constant lies in the space $\tau \in \mathcal{T} = \{\tau_0, \ldots, \tau_M\}$, where $\tau_0, ..., \tau_M$ represent the set of admissible time constants.

Based on these considerations, the combined sizing and energy-management can be reformulated as:

$$(n_{bat}^*, n_{sc}^*, \tau^*) = \underset{n_j\in\mathcal{N}_j, \tau\in\mathcal{T}}{\operatorname{argmin}} J_{ins} + J_{run}$$
$$s.t.\ (20), (21)$$

Notice that, by fixing n_j and τ all the variables in the previous problem (powers, currents, voltages, etc.) can be precalculated. Thus, with this pragmatic approach, the search space for the problem is reduced to a 3-dimension domain $\mathcal{N}_{bat} \times \mathcal{N}_{SC} \times \mathcal{T}$.

Remark 1: The original sizing problem (20) is an infinite-dimensional optimization problem, e.g., we must find the ESS's currents $i_j(t)$ throughout the driving cycle. On the other hand, the pragmatic approach proposed here reduces the sizing task to a finite-dimensional optimization problem, i.e., the decision variables are defined by a 3-dimension vector (n_{bat}, n_{sc}, τ). The decrease in computational times needed for extracting the optimal solution is the main advantage in this finite-dimensional optimization problem. As result, complex powertrain and ESS models can be easily integrated in the sizing task. However, it is also important to have in mind that, due to the assumption of a filter-based power split, this pragmatic approach only provides sub-optimal results.

IV. Comparative Results

The aforementioned sizing methodology was applied to design a hybrid ESS for the uCar vehicle, detailed in [3]. In order to investigate the effect of the vehicle's range in the ESS, the US06 cycle was repeated up to 6 times. Additionally, besides sizing the hybrid ESS, we also designed an ESS using only batteries cells, named battery-only solution hereafter. In both cases, the sizing task was carried out using all types of battery models. It was assumed $N_{cycles} = 1500$ trips with an energy cost of $C_e = 0.18$ [\$/kWh]. The characteristics of the cells can be extracted from Tables I and II.

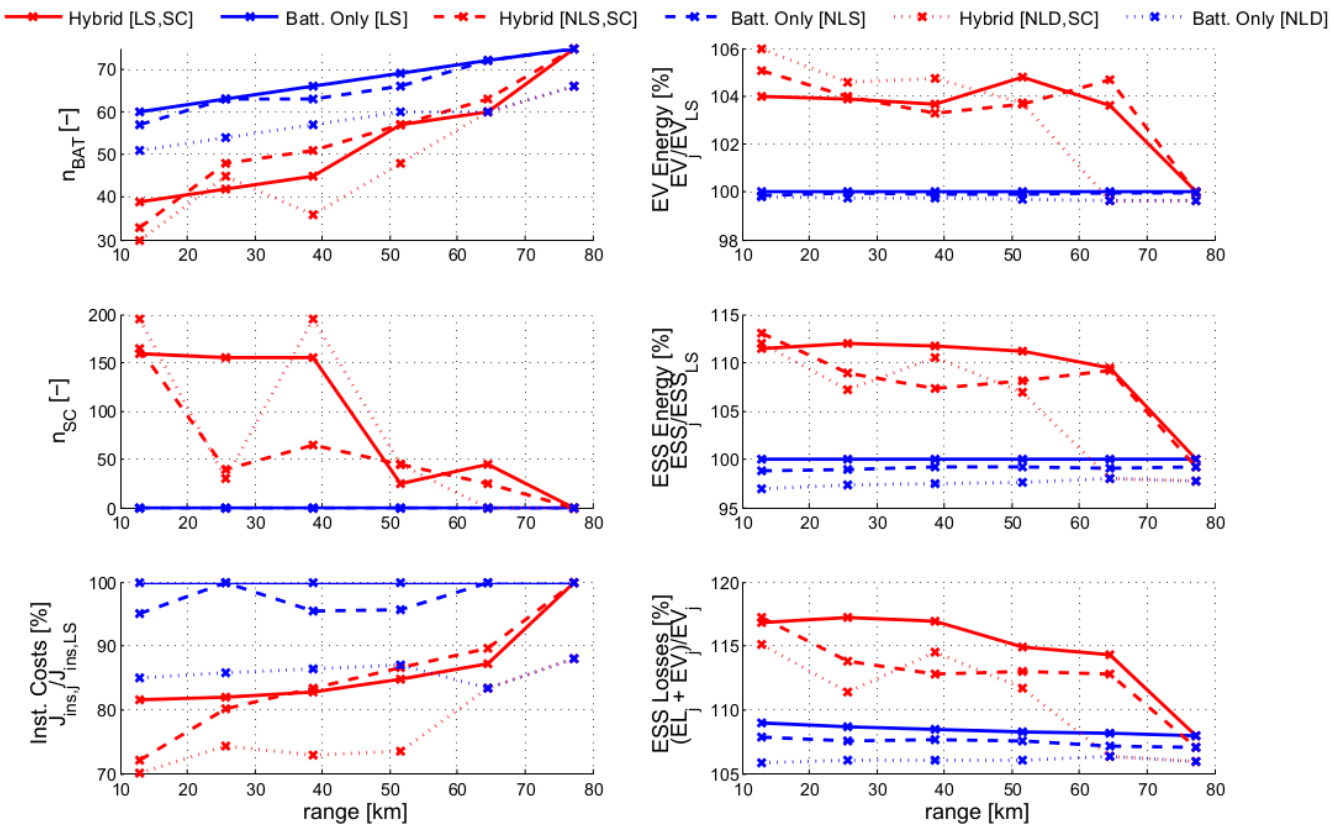

Fig. 4: Performance comparison between different ESS: i) battery only, ii) hybrid ESS, using the filter based strategy. The sub-index $j \in \{LS; LS, SC; NLS; NLS, SC; NLD; NLD, SC\}$.

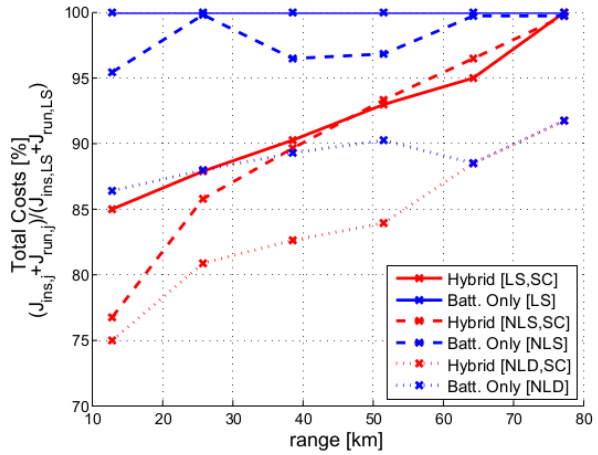

Fig. 3: Total cost comparison between different ESS: i) battery only, ii) hybrid ESS, using the filter based strategy.

A. *Influence of Driving Cycle's Length*

Fig. 3 and 4 presents the sizing results for different ranges of US06 cycle. To facilitate the comparison between different ESS's, the results were normalized relatively to the battery-only solution obtained with the LS model (the plotting of the number of cells is the only exception to this normalization). From these results, one can find a general trend, which is independent of the battery model employed in the sizing. More specifically, if the vehicle's range is not very high, the hybrid ESS is able to provide considerable cost reductions, e.g. between 15 to 25% for a range demand of 12.9km (see Fig. 3). On the other hand, as the vehicle's ranges increases, the economic benefit vanishes; in fact, for ranges higher than 80km, the hybrid ESS converges to the battery only solution (see n_{SC} and n_{Bat} depicted in Fig. 4). The reason for this trend can be explained by the following: with the increase of the vehicle's autonomy, the energy demands will increase to a point (77.3km in our case) where the batteries will be the only necessary source to accomplish both energy and peak power requirements. Furthermore, NLD model presents smaller battery solutions, for every range, compared to the other models, which demonstrates that the simpler models have underrated power capabilities.

Another aspect worth highlighting is the total energy consumption of the vehicle. From the results depicted in Fig. 4 one can observe that the energy consumption and losses of the hybrid ESS increase in comparison with the battery-only solution. There are two reasons for this energy increase. First, the battery-only solution employs a higher number of cells, which contributes to a reduction in the Joule losses (of the

equivalent cell model). The second reason is related with the power allocation strategy, i.e., the filter-based approach used to split the power in the hybrid ESS does not provide globally optimal solutions (see also Remark 1). In any case, these results suggest that, while offering a reduction in the total costs (installation + running), the hybrid ESS may reduce the energy-efficiency of the storage unit.

B. Influence of Battery Models

As already mentioned, one of the main goals of this paper is to evaluate the effect of battery models in the sizing of ESS's. With this goal in mind, let us analyse in more detail the sizing of the battery-only solution. From Fig. 4, it can be observed that increasing the model complexity the required number of cells is reduced. However, the difference between the models is not uniform; in fact, the results are affected by the range requirements of the vehicles. For example, for a range of 12.9km, the battery-only (LS) requires 60 cells, while the NLS uses 57 and NLD uses 51, i.e. 6% and 18% reduction in the number of cells, respectively (and approximately 5% and 14% in the total cost). On the other hand, for a ranges above 60km there are no differences between LS and NLS. These results suggest that the use of a simple LS models and even NLS may generated, in some cases, oversized (battery-only) storage units. The main reason for these results is the dynamic effect of the batteries. For example, in a discharge step, the battery's terminal voltage of the NLD model, decays with a time constant given by $R_1(q(t))C_1(q(t))$, while the LS and NLS models have an instantaneous voltage drop. This means that, for the same required (discharge) power, the peak currents in the NLD model are inferior to the LS and NLS models, leading to a lower amount of cells.

Interestingly, the same behaviour is observed in the sizing of the hybrid ESS, i.e., the LS and NLS models generally produce over-sized storage units. This claim is particularly visible for ranges demands above 25km. As an example for 39km with LS model we need $n_{Bat} = 45$, $n_{SC} = 155$, $J_{Cost} = 90.3\%$, while the NLS model generates $n_{Bat} = 48$ (more 7%), $n_{SC} = 65$ (less 58%) and $J_{Cost} = 89.6\%$ (less 1%) and the NLD model generates $n_{Bat} = 36$ (less 20%), $n_{SC} = 195$ (more 26%) and $J_{Cost} = 82.6\%$ (less 8%). This observation is further supported by the sizing cost depicted in Fig. 3, i.e., the hybrid ESS with NLD model requires lower costs than the the LS and NLS.

V. Conclusion

This paper presented a comparative study of the influence of different aggregated electrical circuit battery models in the sizing process of a hybrid energy storage system (ESS). Toward that goal a sizing methodology based in low/high pass filters for the power allocation in the ESS was proposed. It was shown that, independently of the battery model, the introduction of SCs in the ESS can provide a significant costs reduction, in some cases higher than 25%. However, this reduction is obtained at the expenses of having higher energy losses, which emphasizes the need to have an optimal power split strategy in the hybrid ESS.

Additionally, the obtained results indicate that, in comparison with the static (linear and nonlinear) battery models, the use of dynamic models in the sizing of hybrid ESS, prevents over-sizing, leading to a decrease in the number of cells (of up to 16% and 29%) and total costs (up to 10% and 9%). According to the study case presented in this paper hybridization of batteries and SCs presents advantages for short driving cycles with high power requirements. Nevertheless, in this sizing strategy, the installation costs only assumed the costs of the cells and the running costs are only based on power losses of the system.

Due to limited space, in this paper, the thermal and ageing aspects of ESSs models, as well the influence of different optimization and power split methods have not been discussed, but will be tackled in future publications.

Acknowledgment

This work is partially funded by FCT, through the scholarship SFRH/BD/90490/2012 and the Danish Strategic Research Council of the project "Advanced Lifetime Predictions of Battery Energy Storage".

References

[1] A. Ravey, B. Blunier, and A. Miraoui, "Control Strategies for Fuel-Cell-Based Hybrid Electric Vehicles: From Offline to Online and Experimental Results," Vehicular Technology, IEEE Transactions on, vol. 61, pp. 2452-2457, 2012.

[2] A. Jaafar, C. R. Akli, B. Sareni, X. Roboam, and A. Jeunesse, "Sizing and Energy Management of a Hybrid Locomotive Based on Flywheel and Accumulators," Vehicular Technology, IEEE Transactions on, vol. 58, pp. 3947-3958, 2009.

[3] R. Araujo, R. de Castro, C. Pinto, P. Melo, and D. Freitas, "Combined Sizing and Energy Management in EVs with Batteries and Supercapacitors," Vehicular Technology, IEEE Transactions on, vol. PP, pp. 1-1, 2014.

[4] C. Pinto, R. de Castro, and R. Esteves Araujo, "A comparative study between causal and non-causal algorithms for the energy management of hybrid storage systems," in Power Electronics and Applications (EPE), 2013 15th European Conference on, 2013, pp. 1-10.

[5] Y. L. Murphey, S. Member, J. Park, Z. Chen, M. L. Kuang, M. A. Masrur, and A. M. Phillips, "Intelligent Hybrid Vehicle Power Control - Part I: Machine Learning of Optimal Vehicle Power", vol. 61, no. 8, pp. 35193530, 2012.

[6] N. Murgovski, L. Johannesson, and J. Sjberg, "Convex modeling of energy buffers in power control applications," in IFAC Workshop on Engine and Powertrain Control Simulation and Modeling, 2012, pp. 92-99.

[7] E. Schaltz, A. Khaligh, and P. O. Rasmussen, "Influence of Battery/Ultracapacitor Energy-Storage Sizing on Battery Lifetime in a Fuel Cell Hybrid Electric Vehicle," Vehicular Technology, IEEE Transactions on, vol. 58, pp. 3882-3891, 2009.

[8] S. G. Wirasingha and A. Emadi, "Classification and Review of Control Strategies for Plug-In Hybrid Electric Vehicles," Vehicular Technology, IEEE Transactions on, vol. 60, pp. 111-122, 2011.

[9] O. Sundstrom, L. Guzzella, and P. Soltic, "Torque-Assist Hybrid Electric Powertrain Sizing: From Optimal Control Towards a Sizing Law," IEEE Transactions on Control Systems Technology, vol. 18, pp. 837-849, 2010.

[10] A. Jossen, Fundamentals of battery dynamics, Journal of Power Sources 154 (2006) 530538.

[11] Chen M. and Rincon-Mora, G. 2006. Accurate electrical battery model capable of predicting runtime and I-V performance. IEEE Trans. Ener. Conv. 21, 2, 504-511.

[12] J. Kowal, J.Bernhard Gerschler, C. Schper, T. Schoenen, D.U. Sauer, Efficient battery models for the design of EV drive trains, 14th International Power Electronics and Motion Control Conference, EPE-PEMC 2010.